Band Gap Modification of TiO$_2$ Nanoparticles by Ascorbic Acid-Stabilized Pd Nanoparticles for Photocatalytic Suzuki–Miyaura and Ullmann Coupling Reactions

Fahimeh Feizpour[1] · Maasoumeh Jafarpour[1] · Abdolreza Rezaeifard[1]

Abstract

In this study, synthesis, characterization and photocatalytic performance of surface-modified TiO$_2$ nanoparticles with ascorbic acid-stabilized Pd nanoparticles are presented. The structure, composition and morphology of as-prepared nanophotocatalyst were characterized by UV-DRS, FT-IR, ICP-AES, TEM and XPS analysis. Ascorbic acid-stabilized Pd nanoparticles induced visible light driven photocatalytic property on the surface of TiO$_2$ which are otherwise insensitive to visible light owing to the wide band gap. The catalytic system worked well for the Suzuki–Miyaura cross-coupling and Ullmann homo-coupling under compact fluorescent light as a visible source with significant activity, selectivity and recyclability. Good to excellent yields of biaryl products were obtained for various aryl halides having different electronic demands and even aryl chlorides. Our results proposed that the improved photoactivity predominantly benefits from the synergistic effects of ascorbic acid-stabilized Pd nanoparticles on TiO$_2$ nanoparticles that cause efficient separation and photoexcited charge carriers and photoredox capability of nanocatalyst. Thus, tuning of band gap of TiO$_2$ making a visible light sensitive photocatalyst, demonstrates a significant advancement in the photocatalytic Suzuki–Miyaura and Ullmann coupling reactions.

Graphical Abstract
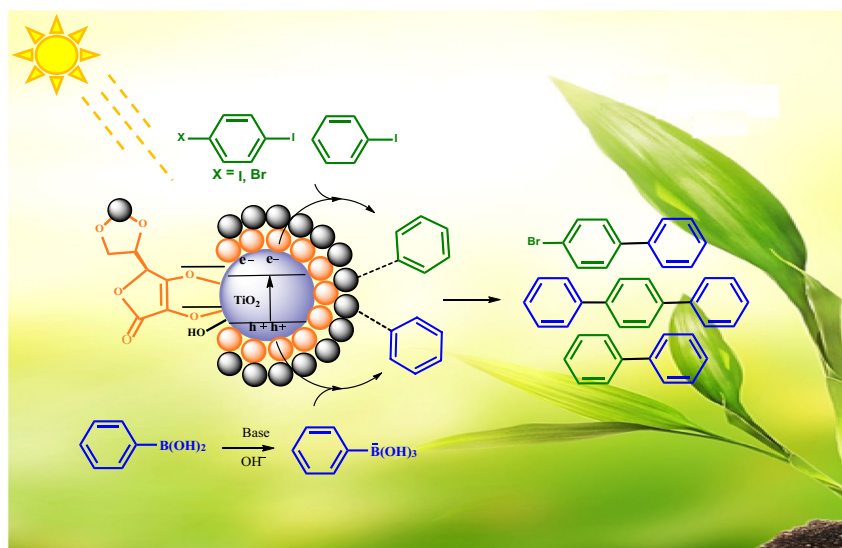
Extended author information available on the last page of the article

 Springer

1 Introduction

In recent years, the search for efficient solar energy conversion has grabbed considerable attention because of rapidly growing energy and environmental concerns [1]. Up to now, metal oxide semiconductors, has emerged as a powerful green tool owning to their potential applications in solar light absorption [2]. In addition, they can be deliberated as part of "green" science, since it lets operating chemical transformations under light irradiation as an environmentally friendly manner [3–6]. Among them, TiO_2 is a promising alternative due to charge carrier handling properties and attractive performance for photochemical applications such as water splitting [7, 8], volatile organic compounds (VOCs) degradation [9], and dye sensitization in solar cell [10, 11], etc. Nevertheless, the wide bandgap of TiO_2 (3.0–3.2 eV) limits its photoactivity to a narrow range of ultraviolet light, i.e. < 4% of sun light [12]. In the quest to enable TiO_2 to absorb a wider spectral range of this abundant natural gift, several research paths have been pursued which makes it archetypical photo catalyst [13–15]. According to limitation of TiO_2, it is significant to tune up band gap energy of TiO_2 to extend photocatalytic property for visible-light-driven photosystem. Toward this end, possible strategy can be done by nanosizing [16, 17], surface grafting (ion doping) [18–20], noble metal nanoparticle deposition [21, 22], co-sensitization [10]. Surface adsorbates including folic acid and enzymes that do not absorb visible light themselves, are among attractive materials for visible light activation of wide band gap semiconductors [23, 24]. Owing to its chemical potential and quick response, ascorbic acid (AA) has been gained attention in this regard [25, 26]. A bathochromic shift up to 600 nm was obtained for the onset of the photoresponse of surface-modified TiO_2 with ascorbic acid [27–30].

Nowadays, technological advancements have led to novel synthetic approaches that are essential to reduce the energy consumption and ecological impact. Interestingly, C–C bond formation using Pd-containing catalyst has garnered attention due to its application in the synthesis of bioactive compound, material and pharmaceuticals science [31–34]. In this direction, the studies on developing efficient catalysts for the given reaction were mostly focused on designing the morphology, structural texture, and catalyst supports of Pd nanocatalyst [31, 35–41].

Following the more efficient Pd-based catalysts which depend on electron richness relative to the activation mechanism [42–44], we are fascinated to improve the efficiency of catalysts involving palladium by increasing their electron density through support effects.

Extensive studies have been dedicated to exert of photocatalysts in photoredox reactions [45, 46]. However, little attention has been developed for carbon–carbon cross and specially homo coupling reaction like Suzuki, Heck and Ullmann type reaction that stay basically untouched from light [47–53].

Further, incorporating electron transfer of photocatalysts with heterogeneous catalysts is actually a novel and promising for chemistry. On the other hand, the design of novel photocatalyst has seen the imperative to derive chemical reaction under visible light irradiation that assist the coupling reaction of less active compound under unexpected conditions.

With this goal in mind as a part of our ongoing project on surface-modification of metal oxides to development of novel strategies for the organic transformation [53–58], we modified band gap of TiO_2 nanoparticles by ascorbic acid-stabilized Pd nanoparticles. Then, the photocatalytic activity of novel TiO_2–AA–Pd was investigated in Suzuki and Ullmann type reaction under visible light as an innocuous mediator in solvent free condition (Scheme 1). Our experiments showed that the improved photoactivity predominantly originated from the synergistic effects of ascorbic acid-stabilized Pd nanoparticles on TiO_2 nanoparticles. The promoted separation and photogenerated charge carriers and photoredox capability of nanocatalyst are important advantages, demonstrating the tuning of the band gap of TiO_2 and its possible application in the visible light region.

2 Experimental

2.1 General Remarks

All chemicals were purchased from Merck and Fluka Chemical Companies. Powder X-ray diffraction (XRD) was performed on a Bruker D8-advance X-ray diffractometer with Cu Kα (λ = 1.54178 Å) radiation.The FT-IR spectra were recorded on NICOLET system. Thermogravimetric analysis (TGA) of nanopowders was performed in the air by Shimadzu 50. TEM images were obtained by TEM instrumentation (Philips CM 10). XP spectra were recorded using a BESTEC GMBH (10^{-10} mw) with Al anode. Diffuse reflectance UV–Vis spectra were recorded using an Avantes spectrometer (Avaspec-2048-TEC model). The Pd content of the catalyst was determined by OPTIMA 7300DV ICP analyzer. Progresses of the reactions were monitored by TLC using silica-gel SIL G/UV 254 plates and also by GC-FID on a Shimadzu GC-16A instrument using a 25 m
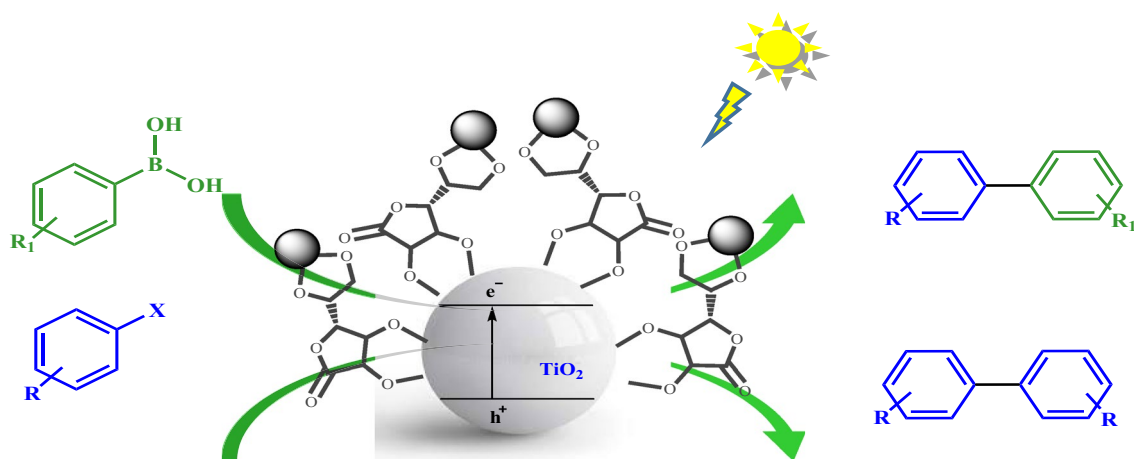
Scheme 1 Suzuki–Miyaura and Ullmann coupling reactions in the presence of TiO$_2$–AA–Pd nanohybrid

CBP1-S25 (0.32 mm ID, 0.5 μm coating) capillary column. NMR spectra were recorded on a BruckerAvance DPX 400 MHz instruments. The dependence of the catalytic performance on the light wavelength was investigated by employing various optical filters to allow the transmission of specific-wavelength light.

2.2 Preparation of TiO$_2$–AA–Pd Nanohybrid

See supporting information.

2.3 General Procedure for Photocatalytic Suzuki–Miyaura Cross Coupling Reactions

In a typical reaction, a mixture of aryl halid (0.2 mmol), arylboronic acid (0.22 mmol), Et$_3$N (0.4 mmol) and TiO$_2$–AA–Pd nano hybrid (0.15 mol%) was added in a 10 mL Pyrex test tube and sealed with septum cap. Then the reaction mixture transferred into a reactor chamber and irradiated under magnetic stirring using a CFL lamp (philips, wavelength in the range 390–750 nm, 40 W, 1.1 W m^{-2}) as the visible light source at 70 °C for appropriate time. After completion of the reaction, TiO$_2$–AA–Pd nanohybrid was extracted by adding of ethanol (5 mL) followed by centrifuging and decantation (3 × 5 mL ethanol). Then, desired product (liquid phase) was extracted by plate chromatography eluted with *n*-hexane/EtOAc (10/2).

2.4 General Procedure for Photocatalytic Ullmann Coupling Reactions

In a typical reaction, a mixture of aryl halid (0.25 mmol), Et$_3$N (0.25 mmol) and TiO$_2$–AA–Pd nanohybrid (0.3 mol%) was added in a 10 mL Pyrex test tube and sealed with septum cap. Then the reaction mixture transferred into a reactor chamber and irradiated under magnetic stirring using a CFL lamp (philips, wavelength in the range 390–750 nm, 40 W, 1.1 W m^{-2}) as the visible light source at 100 °C for appropriate time. After completion of the reaction, TiO$_2$–AA–Pd nanohybrid was extracted by adding of ethanol (5 ml) followed by centrifuging and decantation (3 × 5 mL ethanol). Then, desired product (liquid phase) was extracted by plate chromatography eluted with n-hexane/EtOAc (10/2).

2.5 Reusability of Catalyst

To a mixture of iodobenzene (1 mmol), phenylboronic acid (1.1 mmol), Et$_3$N (2 mmol) was added TiO$_2$-AA-Pd nanohybrid (0.6 mol%) and the reaction mixture transferred into a reactor chamber and irradiated under magnetic stirring using a CFL lamp, at 70 °C for a certain period of time. After completion of the reaction, the TiO$_2$-AA-Pd nanohybrid was recycled by adding of ethanol (5 mL) followed by centrifuging and decantation (3 × 5 mL ethanol). The isolated solid phase (TiO$_2$–AA–Pd nanohybrid) was dried under reduced pressure and reused for next runs. Catalyst recovery was also investigated in the Ullmann coupling reaction according to the above mentioned procedures.

3 Results and Discussion

3.1 Catalyst Fabrication and Characterization

TiO$_2$ and TiO$_2$–AA nanohybrid were prepared and purified following the literature (for experimental details see SI). As described in Scheme S1, TiO$_2$–AA–Pd nanohybrid was synthesized by incorporating of Pd(OAc)$_2$ into ascorbic acid decorated on TiO$_2$ nanoparticles that has been dispersed in ethanol under ultrasonic agitation. The as-prepared

TiO$_2$–AA–Pd was analyzed by ICP-AES and revealed that the contents of Pd was 0.2 mmol g^{-1} (2.12 wt%).

Figure 1 shows the FT-IR spectra of (a) TiO$_2$, (b) TiO$_2$–AA, and (c) TiO$_2$–AA–Pd nanocatalyst. The major bands at 450–775 cm^{-1} present in all samples are assigned to the stretching vibrations of Ti–O groups [59, 60]. In Fig. 1a, broad peaks at 3400 and 1629 cm^{-1}, correspond to the surface adsorbed water and hydroxyl groups. Figure 1b confirms the successful fabrication of TiO$_2$/AA composite. Furan ring of AA with vicinal hydroxyl groups acts in a bidentate chelating mode with Ti atoms [61]. C–O stretching vibration of Ti–O–C is appeared in the range of 927 and 1010 cm^{-1} [62]. The strong peak at 1320 cm^{-1} assigned to the O–H enediol of free acid, disappeared after complexation indicating the coordination of the O$_{C3}$ and O$_{C2}$ atoms to the Ti centers [63]. Figure 1c demonstrates significant spectral changes in the FT-IR spectra of TiO$_2$/AA/Pd compared to those of TiO$_2$ and TiO$_2$/AA (Fig. 1a, b). A new weak band at 498 cm^{-1} is appeared and other bands shift to higher wavenumbers, evidences for Pd coordinated by AA coated TiO$_2$ [Pd–O bond] [64].

To investigate the chemical state of Pd species, XPS measurements were employed in the region from 0 to 1100 eV (Fig. 2). The peak of C 1s is assigned at 285 eV and calibrated by taking as reference. The peaks corresponding to oxygen [O 1s (530 eV)], carbon (C 1s), and Ti 2p$_{3/2}$ and Ti 2p$_{1/2}$ [459 and 464 eV] [65–67] are also distinctly elucidated in the survey XPS spectrum of the TiO$_2$–AA–Pd nanohybrid. As seen in Fig. 2c, the binding energies of Pd 3d$_{3/2}$ and 3d$_{5/2}$ in the nanohybrid were 340.54 eV and 335.3 eV, respectively, [68] which revealed that Pd(0) was present.
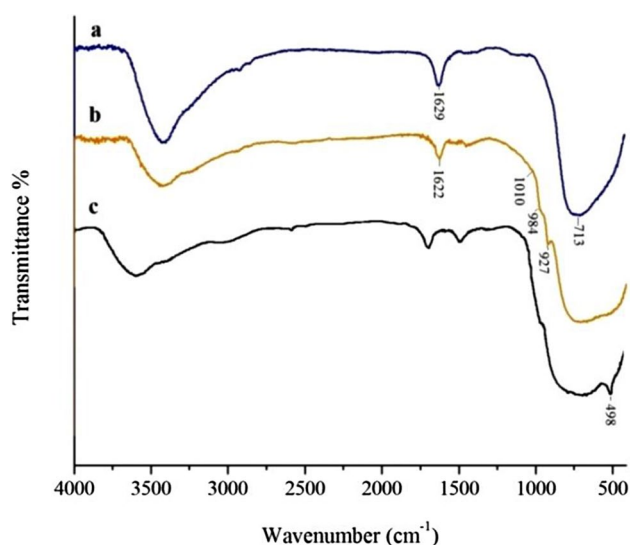
Fig. 1 FT-IR spectra of **a** nanostructure TiO$_2$, **b** TiO$_2$–AA, **c** TiO$_2$–AA–Pd nanohybrid

The morphology of catalyst was screened by TEM measurement and the images are presented in Fig. 3. A uniform distribution of spherical nanoparticles with size ranging between 15 and 20 nm can be ascribed to TiO$_2$–AA–Pd prepared in this work.

3.2 Catalyst Screening in Suzuki Cross-Coupling Reaction

Initially, to check the potential of TiO$_2$–AA–Pd nanohybrid for catalyzing the Suzuki–Miyaura coupling reaction, the reaction between iodobenzene (0.2 mmol) and phenylboronic acid (0.22 mmol) was chosen as a model reaction. To achieve the desired conditions, various factors including the nature of solvent and base, catalyst loading, and temperature were screened (Fig. S1). According to the results presented in Fig. S1i, removing the solvent improved the yield of biphenyl, then a solvent-free condition was chosen for the reaction (Fig. S1i). Among different bases tested here, Na$_2$CO$_3$ was a poor one for the coupling and K$_2$CO$_3$, KOH, KF and NaOH gave moderate yields. Nevertheless, the use of 0.4 mmol Et$_3$N as an organic base led to higher performance of this reaction and consequently, hereafter it will be used (Fig. S1iii). Next we addressed to optimize the catalyst loading. A quantitative yield of the desired product was achieved at 70 °C in the presence of 0.15 mol% TiO$_2$–AA–Pd nanohybrid after 1 h. Decreasing the catalyst loading to 0.1 and 0.07 mol% reduced the yields to 70 and 40%, respectively (Fig. S1iv).

On the basis of the above mentioned experiments, after 1 h reaction at 70 °C, the quantitative yield of 95% of biphenyl was obtained, in the presence of 0.15 mol% TiO$_2$–AA–Pd nanohybrid, 0.4 mmol Et$_3$N under solvent-free conditions and visible light irradiation (Table 1, entry 1). It is noteworthy that, in the absence of iodobenzene no evidence for self-coupling of phenylboronic acid was observed under optimized conditions.

The scope of the reaction was studied with electronically and structurally diverse aryl halides with different substituted arylboronic acids (Table 1). Desired activities were observed for arylhalides even aryl chlorides as deactivated arylhalides, giving the corresponding biphenyl compounds in good to excellent yields within 0.5–6 h under the optimized reaction conditions (Table 1).

More investigations sought to understand the impact of the halides (I, Br, Cl) of arylhalides. When aryliodides (entries 1–5) were replaced by bromide counterparts (entries 6–9), the trends in reactivity remained almost unchanged, nevertheless, reactions took longer. As an example, when iodobenzene or bromobenzene subjected to the same reaction conditions, biphenyl as a Suzuki coupled product formed in 95 and 90% yield within 1 and 4 h respectively. Furthermore, the least reactivity for the coupling reaction
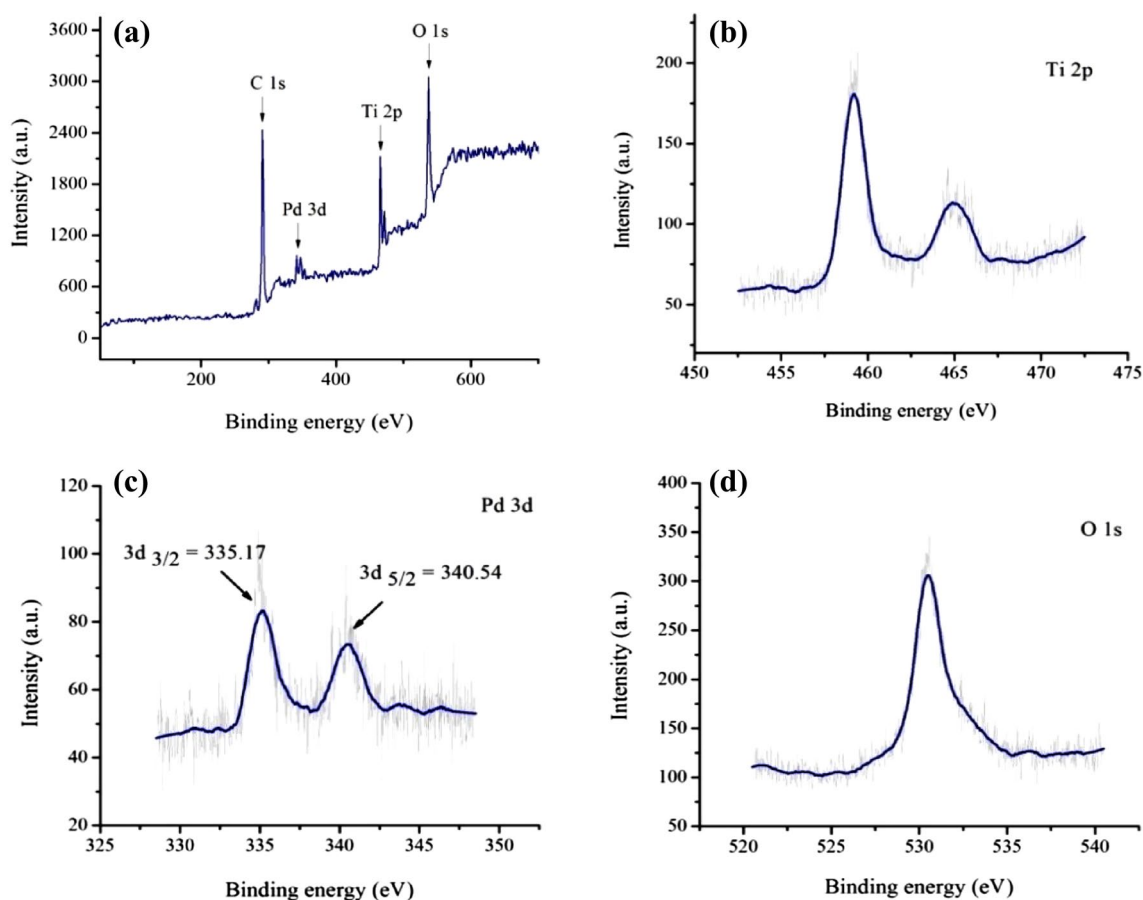
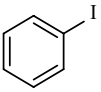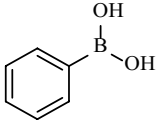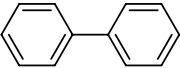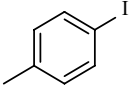**Fig. 2** XPS spectra of TiO$_2$–AA–Pd nanohybrid **a** wide scan, **b** Ti 2p, **c** Pd 3d, and **d** O 1s
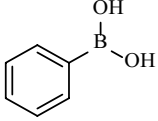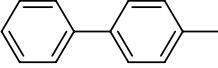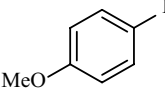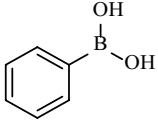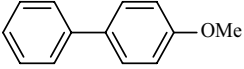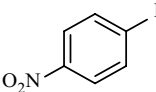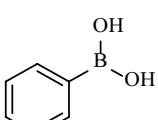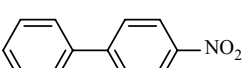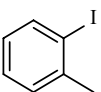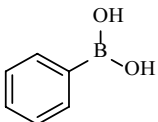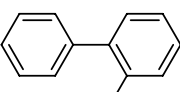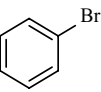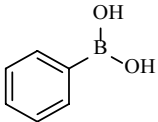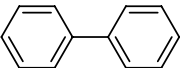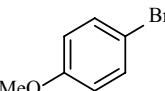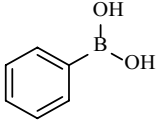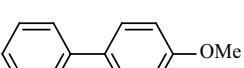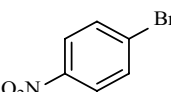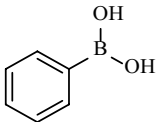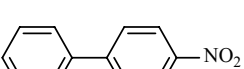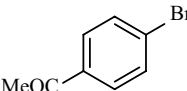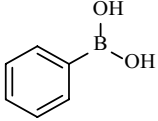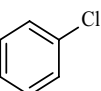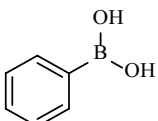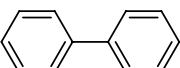
Fig. 3 TEM of TiO$_2$–AA–Pd nanohybrid
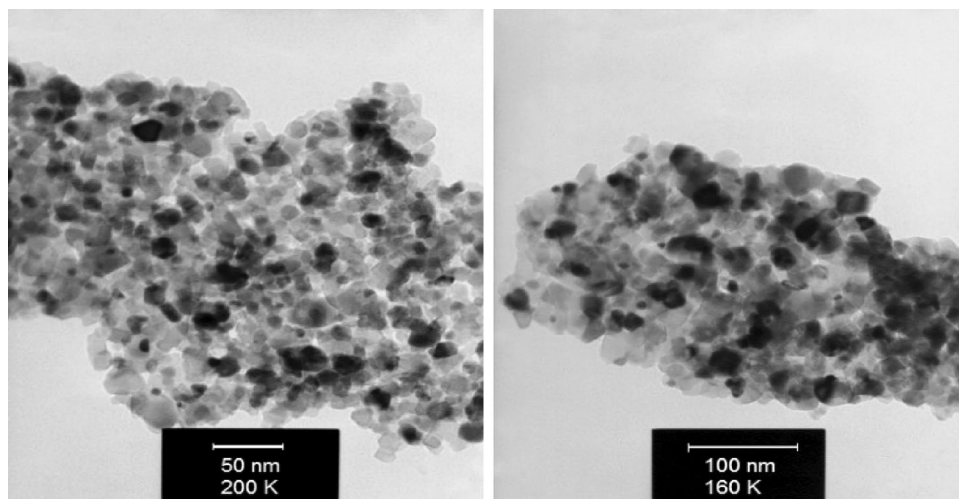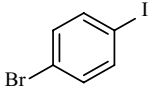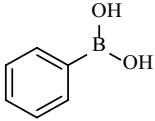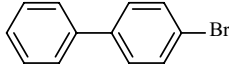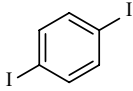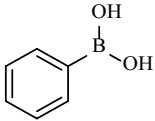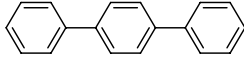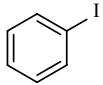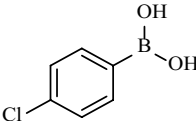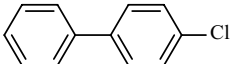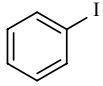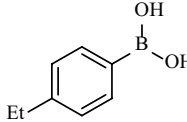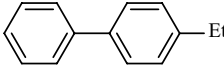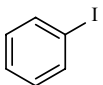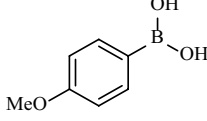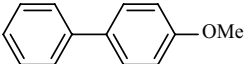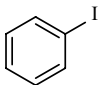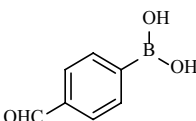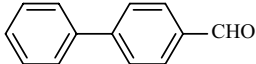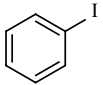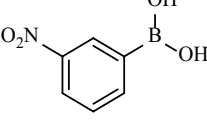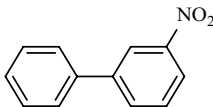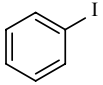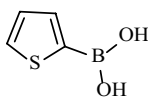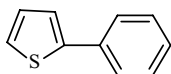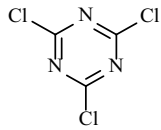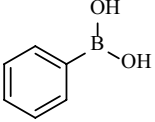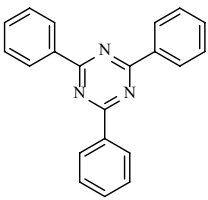
belonged to chlorobenzene, as expected (entry 10, 80% in 6 h). This reactivity order (Cl < Br < I) reflects the strength of the C–X bond leading to the conclusion that alkyl iodides are the most reactive members of this functional class for C–C bond formation. According to the data in entries 3, 4, 7, 8 and 9 in Table 1, electron-rich and electron-poor aryl halides were al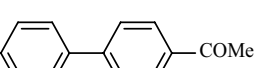so appropriate substrates to give the pertinent unsymmetrical coupling products in 82–96% isolated yields. Moreover, excellent activity was observed with electron-poor aryl halides with good functional group tolerance

Table 1 The Suzuki–Miyaura cross coupling using TiO$_2$–AA–Pd

Entry	Aryl halide	Aryl boronic acid	Product[a]	Time (h)	Yield (%)[b]
1				1	95
2				1	90
3				2	84
4				0.5	96
5				1.5	90
6				4	90
7				5	82
8				3	94
9				4	90
10				6	80

Table 1 (continued)

Entry	Aryl halide	Aryl boronic acid	Product[a]	Time (h)	Yield (%)[b]
11				2	90
12[c]				2	71
13				2	90
14				2	81
15				2.5	85
16				2	90
17				4	45
18				2	70
19[d]				6	70

Reaction conditions: arylhalides (0.2 mmol), arylboronic acid (0.22 mmol), TiO$_2$–AA–Pd (0.15 mol %), Et$_3$N (0.4 mmol) under visible light irradiation (CFL, 40 W), air and solvent free conditions at 70 °C

[a]The products were identified by comparison with authentic samples and ^{1}H NMR spectroscopy

[b]Isolated yield

[c]Substrate ratio 1:2

[d]In DMF solvent, substrate ratio 1:3, (25% yield obtained under solvent free conditions)

(entries 4, 8, 9). For example, coupling of 4-nitro derivative aryl iodide or aryl bromide with phenylboronic acid, gave the related 4-nitrobiphenyl with the yield of 96 and 94% in 0.5 and 3 h, respectively. Whiles, cross coupling of methoxy derivative aryl iodide or aryl bromide with phenylboronic acid produced 4-methoxybiphenyl in 84 and 82% yields in 2 and 5 h, respectively. Nevertheless, when phenylboronic acid substituted with various groups, no such significant effect was found in the yield and the rate of the Suzuki coupling reaction (Table 1, entries 13–18) expect for 3-nitro phenylboronic acid and 2-thiophene boronic acid.

It is notable that the bihalide containing I and Br reacted with high efficiency meanwhile, selectivity well conducted between reactive halides (entry 11). Moreover, one-pot double couplings of 1,4-diiodobenzene and phenylboronic acid occurred to produce a desired yield of terphenyl (71%) in 2 h (entry 12). Aryl 1,3,5-triazine derivatives have attracted considerable interest because of its appealing performance in herbicide [69], suitable ligands for providing of liquid crystals [70], material science and hydrogenation of various compounds [71]. However, one pot multiple Suzuki coupling reaction can be more challenging to such 1,3,5-triazine derivatives. When triazine was reacted with phenylboronic acid under optimized conditions of this work, only 25% of 2,4,6-triphenyl-1,3,5-triazine was formed. Nontheless, performing the reaction in DMF at 70 °C improved the yield of produt to 70% after 6 h (entry 19). Needless to say, reducing the steps of reaction to access to fully aryl-substituted arenes is a salient feature of this work which is a necessity for the Suzuki coupling reaction.

3.3 Ullmann Coupling Reactions

During the optimization of temperature in the Suzuki–Miyaura reaction based on model reaction, we observed a by-product. So, we decided to evaluate self-coupling of phenylboronic acid and iodobenzene in the absence of each other at higher temperature under solvent free conditions. In different conditions, the pertinent product of self-coupling of phenylboronic acid was not detected but at higher temperature, self-coupling of iodobenzene occurred under solvent-free condition.

Encouraged by these results we tried to explore a heterogeneous photothermal system for the Ullmann type reaction of arylhalides. Biphenyl was achieved from homocoupling reaction of iodobenzene after 4 h when 0.3 mol% TiO$_2$–AA–Pd and 0.5 mmol Et$_3$N was mixed under solvent free conditions at 100 °C (Fig. S2 in SI). The good to high yields (65–95%) as well as excellent selectivity (> 99%) were obtained in the homocoupling reaction of arylhalides (Table 2).

As seen in Table 2, a structurally diverse aryl halides involving electron-rich and electron-deficient groups were subjected to homocoupling reactions. The reactions proceeded well under catalytic influence of a low catalyst loading of 0.3 mol% TiO$_2$–AA–Pd to give corresponding biaryls in 65–95% yield.

Like Suzuki–Miyaura coupling reactions aryl bromides and chlorides (Table 2, entries 6–10) are less reactive than those of the related aryl iodides in the Ullmann type homocoupling reactions. Screening the electronic demands on the reaction performance, *para*-substituted halobenzenes were tested. Regardless of halobenzene's substitution, both electron-poor and electron-rich substrates reacted smoothly affording biphenyl products in good to excellent yields in 3–10 h. Apparently, the reaction with electron-rich aryl halides was significantly slower with less yield under the similar reaction conditions. Finally, chemoselectively was remarked. In this direction, 1-bromo-4-iodobenzene as a model substrate was coupled exclusively, at iodine position (Table 2, entry 10).
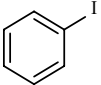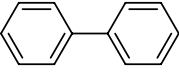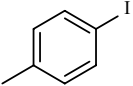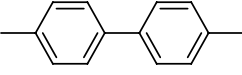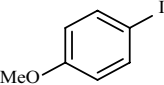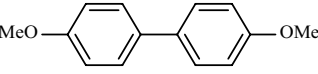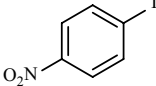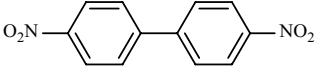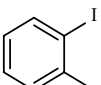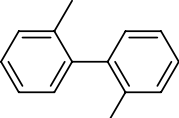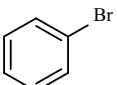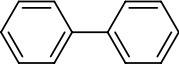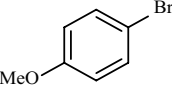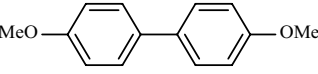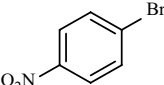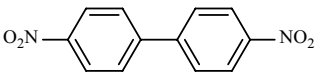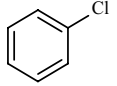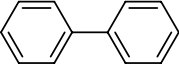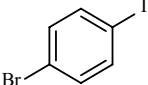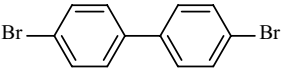
3.4 Photocatalytic Activity

Following our investigation on photochemical properties of surface-modified TiO$_2$ with cobalt(II) [or Fe(III)] ascorbic acid complex [54, 55], herein, the influence of Pd ascorbic acid complex is screened to explain the photoactivity of prepared catalyst under visible-light irradiation. Initially, we replaced the TiO$_2$ core by MoO$_3$ and γ-Fe$_2$O$_3$ to investigate the core dependence of the catalytic activity. Significant reduction in product yield was observed in the cross-coupling reaction between iodobenzene (0.2 mmol) and phenylboronic acid (0.22 mmol) under the same conditions. (Fig. 4). Thus, the photocatalytic activity depends greatly on TiO$_2$ core and affected to the catalytic performance of TiO$_2$–AA–Pd nanohybrid (Fig. 4).

Conducting the reaction in dark condition decreased the product yield to 35% demonstrating that the light absorption by the TiO$_2$–AA–Pd photocatalyst can facilitate the Suzuki cross-coupling reaction. Thus, the photocatalytic activity depends greatly on TiO$_2$ core and affected to the catalytic performance of TiO$_2$–AA–Pd nanohybrid (Fig. 5).

To determine the relative contribution of thermal and photochemical processes, the Suzuki and Ullmann type reaction, were conducted under dark as well as different wavelength ranges of irradiation. Subtracting the conversion in the dark (contribution of thermal effect) from the overall conversion under light gave contribution of light to the conversion efficiency (Fig. 6). To achieve mentioned wavelength ranges, a series of optical low-pass filters were employed to block light below a specific cutoff wavelength. For example, the 450 nm optical filter blocks the wavelength below 450 nm and over 800 nm, in other words, the light irradiating the reactor has a wavelength range from 450 to 800 nm. Without any filters, the

Table 2 The Ullmann coupling reactions of aryl halides using TiO$_2$–AA–Pd

Entry	Aryl halide	Product[a]	Time (h)	Yield %[b]
1			4	95
2			5	90
3			5	75
4			3	90
5			5	65
6			6	85
7			7	74
8			7	82
9			10	65
10			5	90

Reaction conditions: arylhalides (0.25 mmol), TiO$_2$–AA–Pd (0.3 mol%), triethylamine (0.5 mmol) under visible light irradiation (CFL, 40 W), air and solvent free conditions at 100 C

[a]The products were identified by comparison with authentic samples and ^{1}H NMR spectroscopy

[b]Isolated yield

irradiation of the light with wavelengths ranging from 400 to 800 nm gives a 4,4-biphenyl yield of 95%. The yield decreases to 80%, 57% and 45% when the wavelength range of the irradiation is 450–800, 550–800, and 600–800 nm, respectively. Since the yield of 4,4-biphenyl in the dark is 35%, the contribution of 400–450 nm light accounts for about 25% ((60 − 45)/60 × 100%) in the total light-induced yield. Similarly, the light in the wavelength range of 450–550, 550–600 and 600–800 nm, respectively accounts for 38%, 21% and 16% of the light-induced yield (Fig. 6a). Also a similar trend was performed for Ullmann coupling reaction.
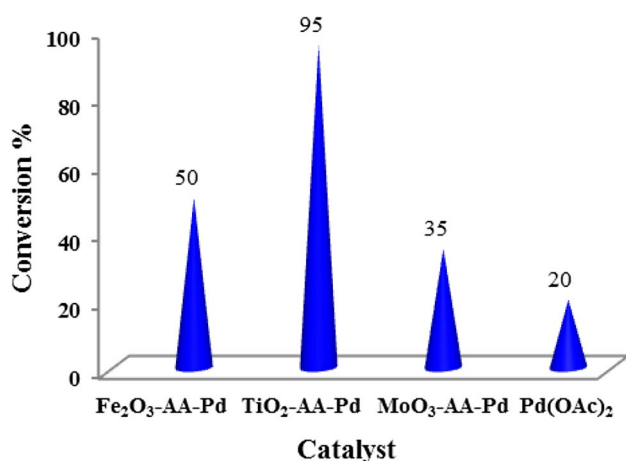
Fig. 4 The comparison of catalytic activity of TiO$_2$–AA–Pd with other nanocatalyst
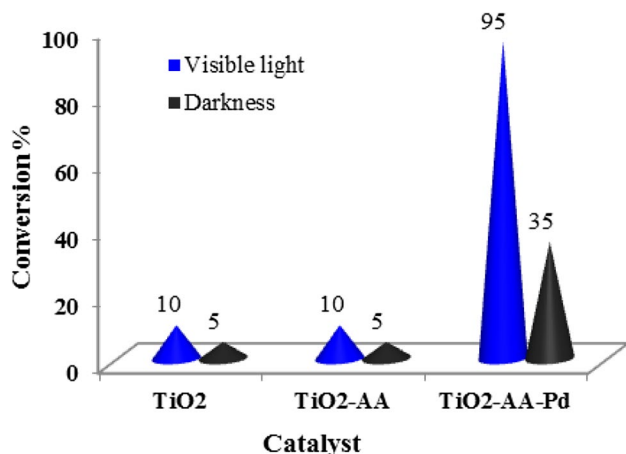
Fig. 5 The screening of photocatalytic activity of TiO$_2$–AA–Pd, TiO$_2$–AA and TiO$_2$ nanoparticle under visible light and darkness condition base on optimized method

Figure 7 shows the action spectra for synthesis of 4,4-biphenyl. The action spectrum is a beneficial manner for identifying whether an observed reaction is caused by photoinduced process or a thermocatalytic process which should represent relevance between the wavelength and the light extinction spectrum [72, 73]. In this regard, the reaction rates of the synthesis of 4,4-biphenyl using TiO$_2$–AA–Pd under irradiation with different wavelengths were investigated. A good correlation between apparent quantum yield (AQY) and the diffuse reflectance spectrum of the TiO$_2$–AA–Pd nanohybrid was observed (Fig. 7) in both the reaction of Suzuki–Miyaura and Ullmann reaction. These results convinced us that the reactions are occurring photocatalytically.

The comparative diffuse reflectance UV–Vis spectra of the TiO$_2$, TiO$_2$–AA and TiO$_2$–AA–Pd nanohybrid are shown in Fig. 8. A red shift was observed in the

absorbance of both surface-modified samples (TiO$_2$–AA and TiO$_2$–AA–Pd) in comparison with pure TiO$_2$. So as-prepared samples exhibited visible light absorption, mainly in the wavelength range of 400–600 nm which signifies its photocatalytic activity under visible-light irradiation. For the TiO$_2$–AA–Pd nanohybrid, the absorption band was found at around 490 nm and 630 nm. Diffuse reflectance UV–Vis using the Kubelka–Munk formula and Tauc plot [74], revealed significant reduction of the band-gap of TiO$_2$–AA–Pd nanoparticles (2.96 eV) compared with those of TiO$_2$–AA (3.1 eV) and especially TiO$_2$ nanoparticles (3.15 eV). It can be observed that the band gap energies for the TiO$_2$–AA–Pd nanohybrid is lower than TiO$_2$ and TiO$_2$–AA. Therefore, ascorbic acid-stabilized Pd nanoparticles modified the band gap of TiO$_2$ inducing it to absorb the visible light.

3.5 Mechanism Study

Control experiments were applied to realize the mechanism of the photocatalyzed coupling reaction. On the basis of the observations from the experiments above ("Photocatalytic Activity" section) and previous studies, we believe the electron–hole pair is generated within the TiO$_2$ nanoparticles modified with ascorbic acid-stabilized Pd nanoparticles upon light irradiation (Fig. 9). To prove this claim, iodobenzene reacted with phenyl boronic acid in the presence of ammonium oxalate (AO) as a hole scavenger and TEMPO as a radical scavenger under light irradiation. The yields of coupling products reduced to 22 and 31%, respectively, much close to results obtained in dark condition regardless the presence or lack of scavengers, attributed to the contribution of thermal effect. These results demonstrated well the light-assisted Suzuki reaction rely on the photogenerated e$^-$ and h$^+$. Therefore, photogenerated e$^-$ transferred onto the Pd nanoparticles can enhance the inherent catalytic activity of Pd and photogenerated h+ can stimulate the C–B bonds of the arylboronic acids.

Taking into account of all these inspections, we propose a plausible mechanism on the basis of the above results and previous reports. As displayed in Fig. 9, Pd nanoparticles can trap the photogenerated e$^-$ due to its electron reservoir capacity. Both the photogenerated e$^-$ and energetic Pd nanoparticles can act as active centers to attack the C–X bond of aryl halide, resulting in facilitating the formation of oxidative addition intermediate with Pd. On the other hand, arylboronic acid can acquire an OH$^-$ in the basic reaction medium to form negative B(OH)$_3^-$ species, which is contribute to the trans-metalation process. Significantly, the h+ can assist in cleaving the C–B bond to produce biaryl–Pd complex. The remaining step, which is called the reductive elimination, should not be affected by the visible light [75].
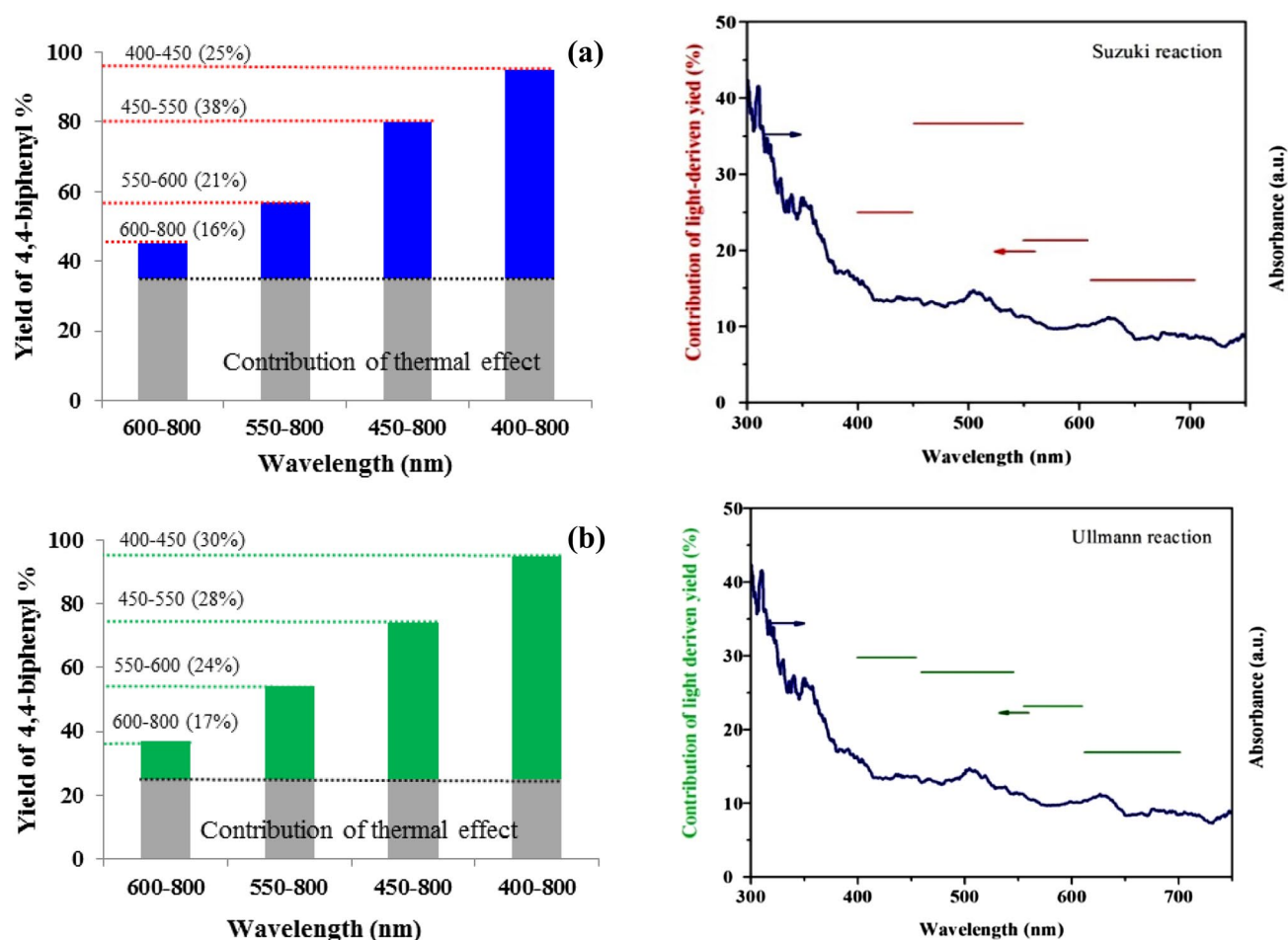
Fig. 6 The dependence of the catalytic activity of TiO$_2$–AA–Pd nanohybrid for **a** Suzuki cross-coupling reaction and **b** Ullmann type reaction on the irradiation wavelength. The numbers in parentheses represent the contribution of the light. Reaction conditions: for **a** iodobenzene (0.2 mmol), phenylboronic acid (0.22 mmol), TiO$_2$–AA–Pd (0.15 mol%), Et$_3$N (0.4 mmol) at 70 °C; **b** arylhalides (0.25 mmol), TiO$_2$–AA–Pd (0.3 mol %), Et$_3$N (0.5 mmol) at 100 °C; under visible light irradiation (CFL, 40 W), air and solvent free conditions

3.6 Stability and Reusability of Catalyst

The TiO$_2$–AA–Pd nanocatalyst can be simply retrieved and reused in the Suzuki–Miyaura cross coupling of model reaction as well as in the Ullmann coupling of iodobenzene. For this purpose, after completing of reactions, ethanol (5 mL) was added to the mixture and then TiO$_2$–AA–Pd nanocatalyst (solid phase) was separated by centrifuging followed by decantation (3 × 5 mL ethanol). The recovered catalyst was washed and reused in six consequent runs in the reactions (Fig. S3). The FT-IR spectrum of the reused catalyst indicates that the structure of catalyst almost completely preserve after recycling (Fig. S4).

To investigate of hot filtration test, we occurred the coupling reactions in DMF as solvent, because product yield under solvent free condition and DMF is the same (Figs. S1, S2). To verify the heterogeneous nature of the title nanocatalyst hot filtration experiments after approximately 50% conversion was carried out, which showed no further increase in the conversion under similar reaction conditions. Then, the filtrate and separated nanocatalyst were analyzed by ICP-AES and no trace of Pd metal was detected, excluding the leaching process and an evidence for stability of catalyst under condition used in this work. Finally, the use of innocuous and abundant visible light energy source, the removing the toxic reagents, or solvents, reusability of catalyst and easy isolation of organic products are further advantageous of the presented methodologies.

Table 3 shows the merit of this operationally photocatalytic protocol in comparison with those previously reported photocatalytic methods, in terms of catalyst loading, yield, and especially, conditions used in the reaction coupling of
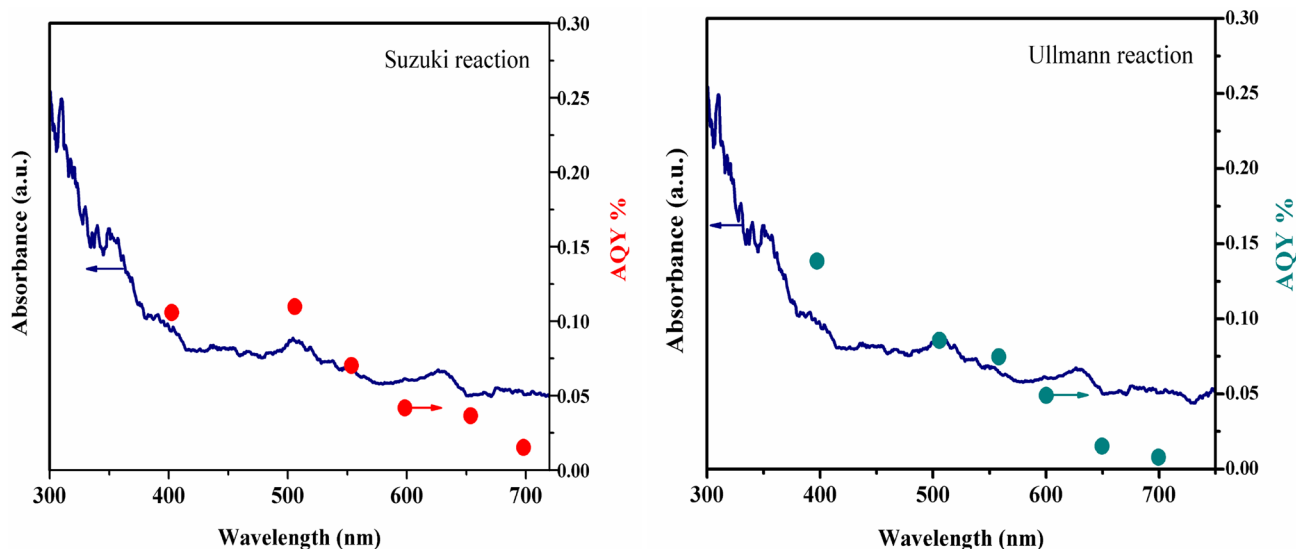
Fig. 7 Action spectrum for synthesis of 4,4-biphenyl using TiO_2–AA–Pd photocatalyst in the Suzuki and Ullmann reaction. The AQY versus the respective wavelengths of the reaction is plotted. AQY was calculated with the following equation: AQY $(\%) = [(Y_{vis} - Y_{dark}) \times 2/$ (photon number entered into the reaction vessel)] $\times 100$, where Y_{light} and Y_{dark} are the amounts of products formed under light irradiation and dark conditions, respectively
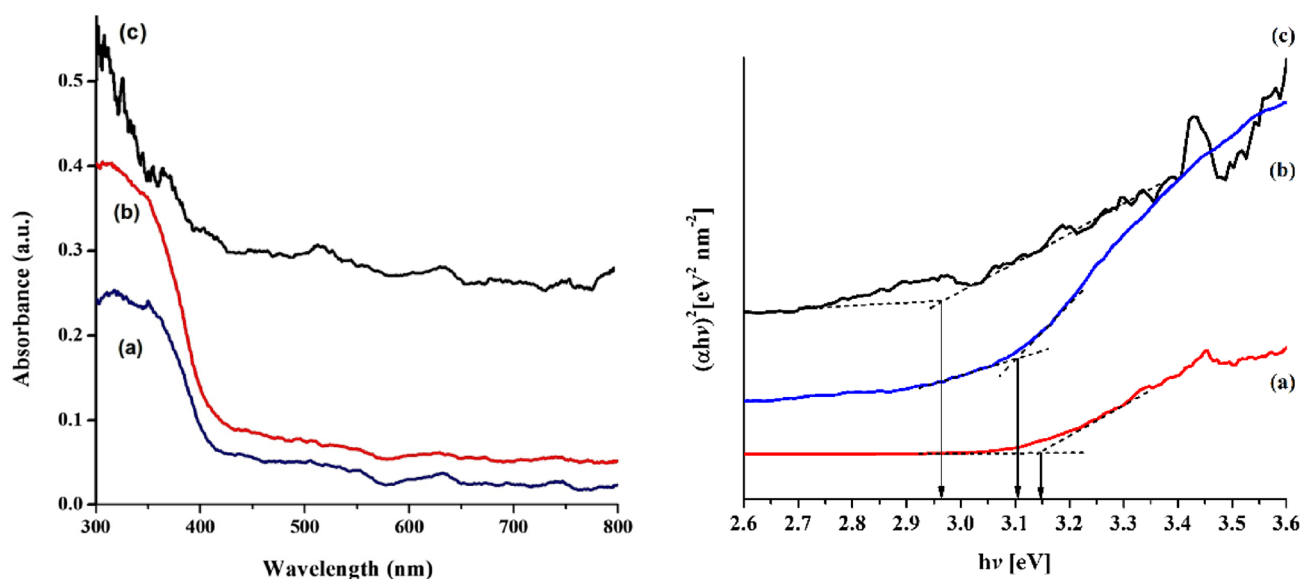
Fig. 8 UV–Vis spectra and DRS of **a** bare TiO_2 NPs, **b** TiO_2–AA and **c** TiO_2–AA–Pd nanohybrid

phenylboronic acid and iodobenzene as model substrate. Therefore, the title methodology is environmentally benign because of using visible light as an innocous energy, reusing of an active catalyst with very low catalyst loading, easy isolation of organic products, and finally, no need for toxic reagents, or solvents.

Fig. 9 Proposed photocatalytic mechanism of carbon–carbon coupling reaction
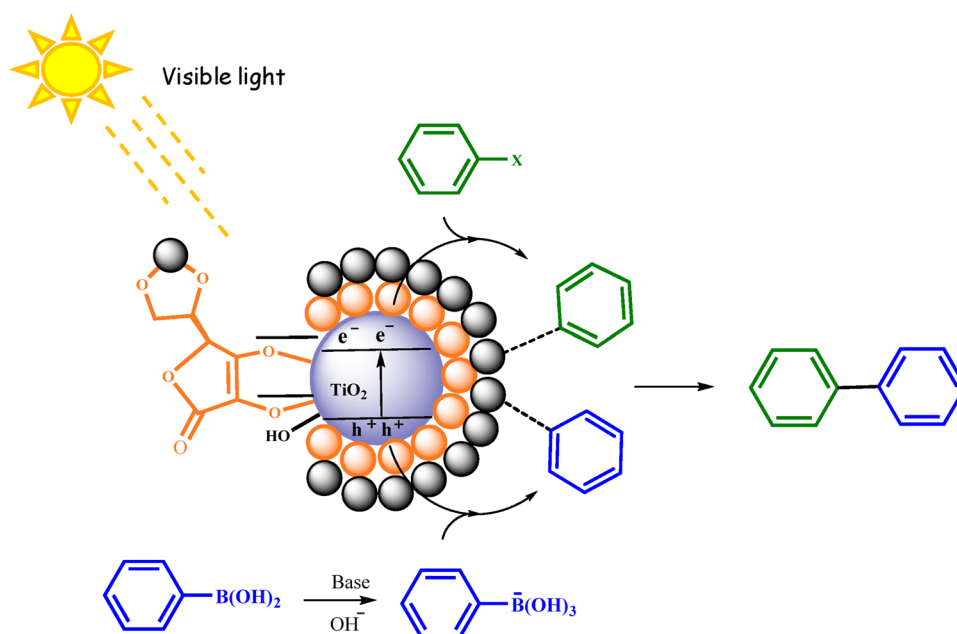
Table 3 Comparison of photocatalytic Pd base catalyst for Suzuki cross coupling reaction using iodobenzene and phenylboronic acid as a substrate

Entry	Catalyst (g)	Condition	Time (h)	Conv. %	Ref.
1	TiO₂–AA–Pd (0.005)	S.F, 70 °C, CFL	1	95	This work
2	Au–Pd alloy NPs (0.05)	DMF/H₂O, K₂CO₃, Ar, 30 °C, incident light	6	98	[72]
3	Pd/TiO₂ (0.7 mol%)	NMP/H₂O, Na₂CO₃, 120 °C	4	97	[75]
4	Pd@MTiO₂ (0.03)	H₂O, K₂CO₃, 70 °C	3	99	[76]
5	Pd/TiO₂ (0.015)	H₂O/PEG, NaOC(CH₃)₃, 28 °C, white LED	4	94	[52]
6	Au–Pd/TiO₂ (0.2 mol%)	H₂O/EtOH, K₂CO₃, 25 °C, blue LED	5	98	[39]
7	Ni-PVPᵃ/TiO₂–ZrO₂ (0.02)	H₂O/MeOH, K₂CO₃, 60 °C	8	97	[77]
8	Pd@B-BO₃ (0.01)	DMF/H₂O, K₂CO₃, rt, white LED	2	98	[78]
9	Pd@PDAᵇ-CL (0.006)	DMF/H₂O, K₂CO₃, rt, white LED	2	96	[49]

[a]Poly(N-vinyl-2-pyrrolidone)

[b]Polydopamine

4 Conclusion

In conclusion, TiO₂–AA–Pd nanohybrid is synthesized by incorporating of Pd(OAc)₂ into ascorbic acid-decorated TiO₂ nanoparticles under ultrasonic agitation. The surface modification with ascorbic acid-stabilized Pd nanoparticles has been induced visible light activity in TiO₂ according to DRS analysis. The title nanophotocatalyst was illustrated to be highly active, selective, and recoverable for the Suzuki–Miyaura cross-coupling and Ullmann homocoupling of a structurally divers of aryl halides including electron-releasing and electron-withdrawing and even aryl chlorides, affording the biaryl compounds in good to excellent yields. The stability of the photocatalyst was evaluated using different manners, indicating that there is virtually no Pd leaching into the reaction solution thus structure of catalyst remained substantially unchanged under reaction conditions. Furthermore, our results represent that the catalytic system can be reused multiple times without significant loss of its activity and stability. It is expected that our work could assign an impressive strategy for making better use of the potential properties of semiconducting materials for various photocatalytic applications.

References

1. Lewis NS, Nocera DG (2006) Powering the planet: chemical challenges in solar energy utilization. Proc Natl Acad Sci 103:15729–15735

2. Rajeshwar K, De Tacconi NR (2009) Solution combustion synthesis of oxide semiconductors for solar energy conversion and environmental remediation. Chem Soc Rev 38:1984–1998

3. Lu B, Li X, Wang T et al (2013) WO_3 nanoparticles decorated on both sidewalls of highly porous TiO_2 nanotubes to improve UV and visible-light photocatalysis. J Mater Chem A 1:3900–3906

4. Amano F, Yamakata A, Nogami K et al (2008) Visible light responsive pristine metal oxide photocatalyst: enhancement of activity by crystallization under hydrothermal treatment. J Am Chem Soc 130:17650–17651

5. Chan SHS, Yeong Wu T, Juan JC, Teh CY (2011) Recent developments of metal oxide semiconductors as photocatalysts in advanced oxidation processes (AOPs) for treatment of dye waste-water. J Chem Technol Biotechnol 86:1130–1158

6. Ravelli D, Dondi D, Fagnoni M, Albini A (2009) Photocatalysis. A multi-faceted concept for green chemistry. Chem Soc Rev 38:1999–2011

7. Ni M, Leung MKH, Leung DYC, Sumathy K (2007) A review and recent developments in photocatalytic water-splitting using TiO_2 for hydrogen production. Renew Sustain Energy Rev 11:401–425

8. Park JH, Kim S, Bard AJ (2006) Novel carbon-doped TiO_2 nanotube arrays with high aspect ratios for efficient solar water splitting. Nano Lett 6:24–28

9. Weon S, Choi W (2016) TiO_2 nanotubes with open channels as deactivation-resistant photocatalyst for the degradation of volatile organic compounds. Environ Sci Technol 50:2556–2563

10. Mor GK, Shankar K, Paulose M et al (2006) Use of highly-ordered TiO_2 nanotube arrays in dye-sensitized solar cells. Nano Lett 6:215–218

11. Liu B, Aydil ES (2009) Growth of oriented single-crystalline rutile TiO_2 nanorods on transparent conducting substrates for dye-sensitized solar cells. J Am Chem Soc 131:3985–3990

12. Chen X, Mao SS (2007) Titanium dioxide nanomaterials: synthesis, properties, modifications, and applications. Chem Rev 107:2891–2959

13. Zhou H, Sun S, Ding H (2017) Surface organic modification of TiO_2 powder and relevant characterization. Adv Mater Sci Eng. https://doi.org/10.1155/2017/9562612

14. Thompson TL, Yates JT (2006) Surface science studies of the photoactivation of TiO_2 new photochemical processes. Chem Rev 106:4428–4453

15. Nolan M, Iwaszuk A, Lucid AK et al (2016) Design of novel visible light active photocatalyst materials: surface modified TiO_2. Adv Mater 28:5425–5446

16. Watson S, Beydoun D, Scott J, Amal R (2004) Preparation of nanosized crystalline TiO_2 particles at low temperature for photocatalysis. J Nanoparticle Res 6:193–207

17. Amano F, Prieto-Mahaney O-O, Terada Y et al (2009) Decahedral single-crystalline particles of anatase titanium (IV) oxide with high photocatalytic activity. Chem Mater 21:2601–2603

18. Anpo M (2000) Use of visible light. Second-generation titanium oxide photocatalysts prepared by the application of an advanced metal ion-implantation method. Pure Appl Chem 72:1787–1792

19. Asahi R, Morikawa T, Ohwaki T et al (2001) Visible-light photocatalysis in nitrogen-doped titanium oxides. Science 293:269–271

20. Zhang Z, Luo Z, Yang Z et al (2013) Band-gap tuning of N-doped TiO_2 photocatalysts for visible-light-driven selective oxidation of alcohols to aldehydes in water. RSC Adv 3:7215–7218

21. Bingham S, Daoud WA (2011) Recent advances in making nano-sized TiO_2 visible-light active through rare-earth metal doping. J Mater Chem 21:2041–2050

22. Xie Y, Ding K, Liu Z et al (2009) In situ controllable loading of ultrafine noble metal particles on titania. J Am Chem Soc 131:6648–6649

23. Zhang G, Kim G, Choi W (2014) Visible light driven photocatalysis mediated via ligand-to-metal charge transfer (LMCT): an alternative approach to solar activation of titania. Energy Environ Sci 7:954–966

24. Houlding VH, Gratzel M (1983) Photochemical hydrogen generation by visible light. Sensitization of titanium dioxide particles by surface complexation with 8-hydroxyquinoline. J Am Chem Soc 105:5695–5696

25. Rajh T, Nedeljkovic JM, Chen LX et al (1999) Improving optical and charge separation properties of nanocrystalline TiO_2 by surface modification with vitamin C. J Phys Chem B 103:3515–3519

26. Ou Y, Lin J-D, Zou H-M, Liao D-W (2005) Effects of surface modification of TiO_2 with ascorbic acid on photocatalytic decolorization of an azo dye reactions and mechanisms. J Mol Catal A 241:59–64

27. Jafarpour M, Feizpour F, Rezaeifard A (2016) Aerobic benzylic C-H oxidation catalyzed by a titania-based organic-inorganic nanohybrid. RSC Adv 6:54649–54660

28. Xagas AP, Bernard MC, Hugot-Le Goff A et al (2000) Surface modification and photosensitisation of TiO_2 nanocrystalline films with ascorbic acid. J Photochem Photobiol A 132:115–120

29. Macyk W, Szaciłowski K, Stochel G et al (2010) Titanium (IV) complexes as direct TiO_2 photosensitizers. Coord Chem Rev 254:2687–2701

30. Yang C, Gong C, Peng T et al (2010) High photocatalytic degradation activity of the polyvinyl chloride (PVC)-vitamin C (VC)-TiO_2 nano-composite film. J Hazard Mater 178:152–156

31. Molnár Á (2011) Efficient, selective, and recyclable palladium catalysts in carbon- carbon coupling reactions. Chem Rev 111:2251–2320

32. Kotha S, Lahiri K (2007) Expanding the diversity of polycyclic aromatics through a Suzuki-Miyaura cross-coupling strategy. Eur J Org Chem 2007:1221–1236

33. Fihri A, Meunier P, Hierso J-C (2007) Performances of symmetrical achiral ferrocenylphosphine ligands in palladium-catalyzed cross-coupling reactions: a review of syntheses, catalytic applications and structural properties. Coord Chem Rev 251:2017–2055

34. Li C-J (2005) Organic reactions in aqueous media with a focus on carbon- carbon bond formations: a decade update. Chem Rev 105:3095–3166

35. Kim S-W, Kim M, Lee WY, Hyeon T (2002) Fabrication of hollow palladium spheres and their successful application to the recyclable heterogeneous catalyst for Suzuki coupling reactions. J Am Chem Soc 124:7642–7643

36. Fihri A, Bouhrara M, Nekoueishahraki B et al (2011) Nanocatalysts for Suzuki cross-coupling reactions. Chem Soc Rev 40:5181–5203

37. Gallon BJ, Kojima RW, Kaner RB, Diaconescu PL (2007) Palladium nanoparticles supported on polyaniline nanofibers as a semi-heterogeneous catalyst in water. Angew Chem Int Ed 46:7251–7254

38. Chen Y-H, Hung H-H, Huang MH (2009) Seed-mediated synthesis of palladium nanorods and branched nanocrystals and their use as recyclable Suzuki coupling reaction catalysts. J Am Chem Soc 131:9114–9121

39. Han D, Bao Z, Xing H et al (2017) Fabrication of plasmonic Au-Pd alloy nanoparticles for photocatalytic Suzuki-Miyaura reactions under ambient conditions. Nanoscale 9:6026–6032

40. Lacerda AM, Larrosa I, Dunn S (2015) Plasmon enhanced visible light photocatalysis for TiO₂ supported Pd nanoparticles. Nanoscale 7:12331–12335

41. Han D, Zhang Z, Bao Z et al (2018) Pd-Ni nanoparticles supported on titanium oxide as effective catalysts for Suzuki-Miyaura coupling reactions. Front Chem Sci Eng 12:24–31

42. Düfert MA, Billingsley KL, Buchwald SL (2013) Suzuki-Miyaura cross-coupling of unprotected, nitrogen-rich heterocycles: substrate scope and mechanistic investigation. J Am Chem Soc 135:12877–12885

43. Fu GC (2008) The development of versatile methods for palladium-catalyzed coupling reactions of aryl electrophiles through the use of P (t-Bu) 3 and PCy₃ as ligands. Acc Chem Res 41:1555–1564

44. Hadei N, Kantchev EAB, O'Brie CJ, Organ MG (2005) Electronic nature of N-heterocyclic carbene ligands: effect on the suzuki reaction. Org Lett 7:1991–1994

45. Tanaka A, Hashimoto K, Kominami H (2012) Preparation of Au/CeO₂ exhibiting strong surface plasmon resonance effective for selective or chemoselective oxidation of alcohols to aldehydes or ketones in aqueous suspensions under irradiation by green light. J Am Chem Soc 134:14526–14533

46. Zheng Z, Huang B, Qin X et al (2011) Facile in situ synthesis of visible-light plasmonic photocatalysts M@TiO₂ (M = Au, Pt, Ag) and evaluation of their photocatalytic oxidation of benzene to phenol. J Mater Chem 21:9079–9087

47. Zhang H, Huang X (2016) Ligand-free Heck reactions of aryl iodides: significant acceleration of the rate through visible light irradiation at ambient temperature. Adv Synth Catal 358:3736–3742

48. Xiao Q, Sarina S, Bo A et al (2014) Visible light-driven cross-coupling reactions at lower temperatures using a photocatalyst of palladium and gold alloy nanoparticles. ACS Catal 4:1725–1734

49. Xie A, Zhang K, Wu F et al (2016) Polydopamine nanofilms as visible light-harvesting interfaces for palladium nanocrystal catalyzed coupling reactions. Catal Sci Technol 6:1764–1771

50. Sarina S, Zhu H, Jaatinen E et al (2013) Enhancing catalytic performance of palladium in gold and palladium alloy nanoparticles for organic synthesis reactions through visible light irradiation at ambient temperatures. J Am Chem Soc 135:5793–5801

51. Lang X, Chen X, Zhao J (2014) Heterogeneous visible light photocatalysis for selective organic transformations. Chem Soc Rev 43:473–486

52. Koohgard M, Hosseini-Sarvari M (2018) Enhancement of Suzuki–Miyaura coupling reaction by photocatalytic palladium nanoparticles anchored to TiO₂ under visible light irradiation. Catal Commun 111:10–15

53. Rezapour E, Jafarpour M, Rezaeifard A (2018) Palladium niacin complex immobilized on starch-coated maghemite nanoparticles as an efficient homo- and cross-coupling catalyst for the synthesis of symmetrical and unsymmetrical biaryls. Catal Lett 148:3165–3177

54. Jafarpour M, Rezaeifard A, Feizpour F (2017) Iron ascorbic acid complex coated TiO₂ nanoparticles enhancing visible-light oxidation performance. ChemistrySelect 2:2901–2909

55. Jafarpour M, Feizpour F, Rezaeifard A (2017) Aerobic stereoselective oxidation of olefins on a visible-light-irradiated titanium dioxide-cobalt-ascorbic acid nanohybrid. Synlett 28:235–238

56. Jafarpour M, Kargar H, Rezaeifard A (2016) A synergistic effect of a cobalt Schiff base complex and TiO₂ nanoparticles on aerobic olefin epoxidation. RSC Adv 6:79085–79089

57. Jafarpour M, Kargar H, Rezaeifard A (2016) A cobalt Schiff base complex on TiO₂ nanoparticles as an effective synergistic nanocatalyst for aerobic C-H oxidation. RSC Adv 6:25034–25046

58. Feizpour F, Jafarpour M, Rezaeifard A (2018) A tandem aerobic photocatalytic synthesis of benzimidazoles by cobalt ascorbic acid complex coated on TiO₂ nanoparticles under visible light. Catal Lett 148:30–40

59. Yang J, Zhang J, Zhu L et al (2006) Synthesis of nano titania particles embedded in mesoporous SBA-15: characterization and photocatalytic activity. J Hazard Mater 137:952–958

60. Pillai SC, Periyat P, George R et al (2007) Synthesis of high-temperature stable anatase TiO₂ photocatalyst. J Phys Chem C 111:1605–1611

61. Rajh T, Nedeljkovic JM, Chen LX, Poluektov O, Thurnauer MC (1999) Improving optical and charge separation properties of nanocrystalline TiO₂ by surface modification with vitamin C. J Phys Chem B 103:3515–3519

62. Ou Y, Lin JD, Zou HM, Liao DW (2005) Effects of surface modification of TiO₂ with ascorbic acid on photocatalytic decolorization of an azo dye reactions and mechanisms. J Mol Catal A 241:59–64

63. Köse DA, Zümreoglu-Karan B (2009) Complexation of boric acid with vitamin C. New J Chem 33:1874–1881

64. Kramareva NV, Stakheev AY, Tkachenko OP et al (2004) Heterogenized palladium chitosan complexes as potential catalysts in oxidation reactions: study of the structure. J Mol Catal A 209:97–106

65. Göpel W, Anderson JA, Frankel D et al (1984) Surface defects of TiO₂ (110): a combined XPS, XAES and ELS study. Surf Sci 139:333–346

66. Cong Y, Zhang J, Chen F, Anpo M (2007) Synthesis and characterization of nitrogen-doped TiO₂ nanophotocatalyst with high visible light activity. J Phys Chem C 111:6976–6982

67. Wang XW, Zhang YQ, Meng H et al (2011) Perpendicular magnetic anisotropy in 70 nm CoFe₂O₄ thin films fabricated on SiO₂/Si (100) by the sol-gel method. J Alloys Compd 509:7803–7807

68. Ivanova AS, Slavinskaya EM, Gulyaev RV et al (2010) Metal-support interactions in Pt/Al₂O₃ and Pd/Al₂O₃ catalysts for CO oxidation. Appl Catal B 97:57–71

69. Menicagli R, Samaritani S, Signore G et al (2004) In vitro cytotoxic activities of 2-alkyl-4, 6-diheteroalkyl-1, 3, 5-triazines: new molecules in anticancer research. J Med Chem 47:4649–4652

70. Yang F, Xie J, Guo H et al (2012) Novel discotic liquid crystal oligomers: 1, 3, 5-triazine-based triphenylene dimer and trimer with wide mesophase. Liq Cryst 39:1368–1374

71. Blotny G (2006) Recent applications of 2,4,6-trichloro-1,3,5-triazine and its derivatives in organic synthesis. Tetrahedron 62:9507–9522

72. Xiao Q, Sarina S, Jaatinen E et al (2014) Efficient photocatalytic Suzuki cross-coupling reactions on Au-Pd alloy nanoparticles under visible light irradiation. Green Chem 16:4272–4285

73. Kowalska E, Abe R, Ohtani B (2009) Visible light-induced photocatalytic reaction of gold-modified titanium (IV) oxide particles: action spectrum analysis. Chem Commun. https://doi.org/10.1039/B815679D

74. Kuvarega AT, Krause RWM, Mamba BB (2011) Nitrogen/palladium-codoped TiO₂ for efficient visible light photocatalytic dye degradation. J Phys Chem C 115:22110–22120

75. Nasrollahzadeh M, Sajadi SM (2016) Green synthesis, characterization and catalytic activity of the Pd/TiO₂ nanoparticles for the ligand-free Suzuki-Miyaura coupling reaction. J Colloid Interface Sci 465:121–127

76. Mondal P, Bhanja P, Khatun R et al (2017) Palladium nanoparticles embedded on mesoporous TiO₂ material (Pd@MTiO₂) as an efficient heterogeneous catalyst for Suzuki-coupling reactions in water medium. J Colloid Interface Sci 508:378–386

77. Kalbasi RJ, Mosaddegh N (2011) Suzuki-Miyaura cross-coupling reaction catalyzed by nickel nanoparticles supported on poly(N-vinyl-2-pyrrolidone)/TiO$_2$-ZrO$_2$ composite. Bull Korean Chem Soc 32:40–44

78. Wang ZJ, Ghasimi S, Landfester K, Zhang KAI (2015) Photocatalytic suzuki coupling reaction using conjugated microporous polymer with immobilized palladium nanoparticles under visible light. Chem Mater 27:1921–1924

Affiliations

Fahimeh Feizpour[1] · Maasoumeh Jafarpour[1] · Abdolreza Rezaeifard[1]

✉ Maasoumeh Jafarpour
mjafarpour@birjand.ac.ir

✉ Abdolreza Rezaeifard
rrezaeifard@birjand.ac.ir; rrezaeifard@gmail.com

1 Catalysis Research Laboratory, Department of Chemistry, Faculty of Science, University of Birjand, Birjand 97179-414, Iran